Superficially-located enlarged lymphoid follicles characterize nodular gastritis

TAKUMA OKAMURA*†, YASUHIRO SAKAI*‡, HITOMI HOSHINO‡, YUGO IWAYA†, EIJI TANAKA†, AND MOTOHIRO KOBAYASHI‡

**Department of Molecular Pathology, Shinshu University Graduate School of Medicine, †Division of Gastroenterology and Hepatology, Department of Internal Medicine, Shinshu University School of Medicine, Matsumoto, and ‡Division of Tumor Pathology, Department of Pathological Sciences, Faculty of Medical Sciences, University of Fukui, Eiheiji, Japan*

Running head: LYMPHOID FOLLICLE HYPERPLASIA IN NODULAR GASTRITIS

Address for Correspondence: Dr. Motohiro Kobayashi, Division of Tumor Pathology, Department of Pathological Sciences, Faculty of Medical Sciences, University of Fukui, 23-3 Matsuoka-Shimoaizuki, Eiheiji, Fukui 910-1193, Japan. E-mail: motokoba@u-fukui.ac.jp Telephone: +81-776-61-8319 / FAX: +81-776-61-8103

Summary

Aims: Nodular gastritis is a form of chronic *Helicobacter pylori* gastritis affecting the gastric antrum and characterized endoscopically by the presence of small nodular lesions resembling gooseflesh. It is generally accepted that hyperplasia of lymphoid follicles histologically characterizes nodular gastritis; however, quantitative analysis in support of this hypothesis has not been reported. Our goal was to determine whether nodular gastritis is characterized by lymphoid follicle hyperplasia.

Methods: The number, size, and location of lymphoid follicles in nodular gastritis were determined and those properties compared to samples of atrophic gastritis. The percentages of high endothelial venule (HEV)-like vessels were also evaluated.

Results: The number of lymphoid follicles was comparable between nodular and atrophic gastritis; however, follicle size in nodular gastritis was significantly greater than that seen in atrophic gastritis. Moreover, lymphoid follicles in nodular gastritis were positioned more superficially than were those in atrophic gastrits. The percentage of MECA-79^{+} HEV-like vessels was greater in areas with gooseflesh-like lesions in nodular versus atrophic gastritis.

Conclusions: Superficially-located hyperplastic lymphoid follicles characterize nodular gastritis, and these follicles correspond to gooseflesh-like nodular lesions observed

endoscopically. These observations suggest that MECA-79^{+} HEV-like vessels could play at least a partial role in the pathogenesis of nodular gastritis.

Key words: Helicobacter pylori, nodular gastritis, lymphoid follicle hyperplasia, high endothelial venule (HEV)-like vessel

INTRODUCTION

Nodular gastritis is a form of chronic *Helicobacter pylori* gastritis characterized endoscopically by the presence of small nodular or granular lesions resembling gooseflesh distributed predominantly in the gastric antrum.[1] Nodular gastritis occurs frequently in children, but there is increasing evidence that nodular gastritis also occurs in adults, particularly in pre-menopausal women.[2-5] Intriguingly, a recent report by Kamada *et al*. demonstrated that, particularly in young women, there is a possible association between nodular gastritis and diffuse-type gastric carcinoma, including signet-ring cell carcinoma.[6] Signet-ring cell carcinoma in advanced stages shows a higher rate of lymph node metastasis and peritoneal dissemination than do other histological types of gastric carcinoma.[7] Thus, it is important to understand the pathogenesis of nodular gastritis and its impact on the development of signet-ring cell carcinoma.

It is generally accepted that histological findings of nodular gastritis include lymphoid hyperplasia, namely hyperplasia of lymphoid follicles.[2,3,8] Shiotani *et al*. noted that biopsy specimens with nodular gastritis tend to contain larger and more superficially-located lymphoid follicles compared to those with atrophic gastritis and hypothesized that follicle size and location are likely related to development of nodular

gastritis.[9] However, those investigators did not perform quantitative histological analysis of the disease.

Lymphoid follicles, a component of mucosa-associated lymphoid tissue (MALT), are believed to be absent from normal stomach.[10] Instead they emerge from chronic antigenic stimulation exerted by *H. pylori* in the gastric mucosa and therefore reflect a specific immune response to this microorganism.[11] Formation of MALT, or lymphoid neogenesis, is thus required for subsequent lymphoid hyperplasia[12] and is elaborated by a multistep process marked by sequential adhesive interactions between circulating lymphocytes and specialized endothelial cells comprising high endothelial venule (HEV)-like vessels.[12-15]

Two adhesion molecules expressed on the luminal surface of HEV-like vessels play a critical role in the initial step of lymphocyte recruitment: peripheral lymph node addressin (PNAd)[16] and mucosal addressin cell adhesion molecule 1 (MAdCAM-1).[17,18] PNAd, a set of sialomucins recognized by the monoclonal antibody MECA-79[19], is constitutively displayed on HEVs in secondary lymphoid organs. Although absent under normal conditions, PNAd is also displayed on HEV-like vessels induced in chronic inflammatory gastrointestinal diseases including chronic *H. pylori* gastritis,[20] ulcerative colitis[21,22] and

autoimmune pancreatitis.[23] The MECA-79 epitope has been shown to be 6-sulfo *N*-acetyllactosamine attached to extended core 1 *O*-glycans, Galβ1→4(sulfo→6)GlcNAcβ1→3Galβ1→3GalNAcα1→Ser/Thr, which overlaps with the L-selectin recognition determinant 6-sulfo sialyl Lewis X (sLeX), sialic acidα2→3Galβ1→4[Fucα1→3(sulfo→6)] GlcNAcβ1→3Galβ1→3GalNAcα1→Ser/Thr.[24,25] MAdCAM-1 belongs to the immunoglobulin superfamily and is constitutively displayed on HEVs in Peyer's patches and mesenteric lymph nodes and on flattened venular endothelial cells in the lamina propria of the intestine, but not seen in the stomach under physiological conditions.[4,26] MAdCAM-1 is an exclusive ligand for integrin α4β7 expressed on memory lymphocytes and functions not only in lymphocyte firm attachment but also in L-selectin-independent lymphocyte rolling in intestinal MALT. Moreover, MAdCAM-1 can be posttranslationally decorated with 6-sulfo sLeX at its mucin-like domain and also supports L-selectin-dependent lymphocyte rolling.[22,27] MAdCAM-1 is thus a dual-function molecule that can serve as a vascular addressin for both L-selectin and α4β7 integrin. Ohara *et al*. has reported that the percentage of MAdCAM-1$^+$ HEV-like vessels in the lamina propria of nodular gastritis is greater than that in control *H. pylori*-positive gastric mucosa.[4] It is also critical to know whether PNAd expression parallels that of MAdCAM-1, since both

molecules may synergize in mucosal lymphocyte homing.[27,28]

In the present study, we determined the number, size, and location of lymphoid follicles, as well as the percentages of MECA-79$^+$ and MAdCAM-1$^+$ HEV-like vessels in nodular gastritis, and compared these properties with those seen in atrophic gastritis and normal gastric mucosa. We found that lymphoid follicles formed in nodular gastritis were more enlarged and superficially located than were those in atrophic gastritis. Hyperplastic lymphoid follicles in nodular gastritis were closely associated with an increased percentage of MECA-79$^+$ HEV-like vessels rather than MAdCAM-1$^+$ HEV-like vessels. These findings indicate that an increase in the percentage of MECA-79$^+$ HEV-like vessels and subsequent formation of superficially-located enlarged lymphoid follicles can serve as histological hallmarks of nodular gastritis.

MATERIALS AND METHODS

Tissue samples

The analysis of human stomach tissues was approved by the Ethics Committee of Shinshu University School of Medicine (protocol numbers 2259 and 2260, approved on April 1st, 2013). Formalin-fixed, paraffin-embedded (FFPE) tissue blocks of gastric biopsy specimens with an endoscopic diagnosis of either nodular (n = 99) or atrophic (n = 65) gastritis were retrieved from the pathological archives of Shinshu University Hospital and its affiliated hospitals. Nodular gastritis was defined endoscopically as an antrum-dominant gastritis with a gooseflesh appearance (Fig. 1A, B), and atrophic gastritis was diagnosed when gastric rugae were flattened and a submucosal vascular pattern was visible in the distended stomach (Fig. 1C). Normal gastric mucosa samples (n = 31) served as controls. In accordance with the updated Sydney system,[29] at least five biopsy specimens were taken from each patient: one each from the lesser (A1) and greater curvature (A2) of the antrum; one from the incisura angularis (IA); and one each from the lesser (B1) and the greater curvature (B2) of the corpus. Patients' clinical characteristics are summarized in Table 1. In all cases, *H. pylori* infection status was determined by a combined histological evaluation and bacterial culture. Of note, one nodular gastritis patient had diffuse-type gastric carcinoma (signet-ring cell carcinoma).

For the integrin α4β7•IgG heterodimeric chimera *in situ* binding assay described below, we obtained fresh gastric mucosa from nodular gastritis patients with informed consent. Fresh tissues were embedded in Tissue-Tek OCT compound (Sakura Finetek, Tokyo, Japan) and frozen at -80°C. Frozen tissues were sectioned at 6 μm, fixed in acetone for 5 min, and briefly air-dried.

Establishment of an anti-human MAdCAM-1 monoclonal antibody

Anti-human MAdCAM-1 monoclonal antibody was generated by ITM Co Ltd (Matsumoto, Japan) basically as described.[30] Briefly, BALB/c mice were immunized with Chinese hamster ovary (CHO) cells stably expressing human MAdCAM-1 (CHO/MAdCAM-1).[22] Two weeks later, lymphocytes obtained from iliac lymph nodes were fused with SP2/0 mouse myeloma cells in the presence of 50% polyethylene glycol (PEG) solution, and cell hybrids were selected for one week in GIT medium (Wako, Osaka, Japan) containing a HAT supplement. After changing the medium to GIT medium containing an HT supplement, cells were cultured another week, and conditioned medium was then screened by immunohistochemistry using FFPE human mesenteric lymph node tissue sections. After several rounds of limited dilution cloning, four hybridoma clones were obtained. We then

used the IsoQuick Kit for Mouse Monoclonal Isotyping (Sigma-Aldrich, St. Louis, MO) to determine that the isotype of all monoclonal antibodies was mouse IgG1κ. Based on its specific reactivity with HEVs in mesenteric lymph nodes (Fig. 2A), clone #15-8G-61 was chosen and used throughout the study. Antibody specificity was confirmed by flow cytometry (Fig. 2B) and Western blot analysis (Fig. 2C).

Immunohistochemistry

The following monoclonal antibodies served as primary antibodies: QBEND10, which recognizes human CD34, a marker of vascular endothelial cells (mouse IgG; Immunotech, Luminy, France); MECA-79, which recognizes 6-sulfo *N*-acetyllactosamine attached to extended core 1 *O*-glycans (rat IgM; BD Pharmingen, San Diego, CA);[19,24] and #15-8G-61, which recognizes human MAdCAM-1 (described above).

Immunohistochemistry for CD34 and MAdCAM-1 was undertaken using the EnVision system (Dako) and that for MECA-79 was carried out using an indirect method described previously.[31]

Quantitative evaluation of lymphoid follicles

We defined a lymphoid follicle as a dense nodular lymphocyte aggregate with or without germinal centers. Using hematoxylin and eosin (H&E)-stained tissue sections, we 1) counted the number of lymphoid follicles in each biopsy specimen and 2) measured the maximal diameter (including mantle zone) of each lymphoid follicle. When possible, we also 3) analyzed occupancy and 4) determined the location of lymphoid follicles in the gastric mucosa with nodular gastritis and atrophic gastritis, as illustrated in Fig. 3. All measurements were carried out at x40 magnification using a BX-51 microscope (Olympus, Tokyo, Japan) and Micro-Ruler for Microscope (Kenis, Osaka, Japan). Histological evaluation was done in a blinded fashion by a single observer (TO) after training by an experienced pathologist (MK).

Quantification of $CD34^+$, $MAdCAM\text{-}1^+$ and $MECA\text{-}79^+$ vessels

The number of respective $CD34^+$, $MAdCAM\text{-}1^+$ and $MECA\text{-}79^+$ vessels in the entire area of each biopsy specimen was determined at x200 magnification under a BX-51 microscope. The number of $MAdCAM\text{-}1^+$ or $MECA\text{-}79^+$ vessels was divided by the number of $CD34^+$ vessels to calculate percentages of $MAdCAM\text{-}1^+$ or $MECA\text{-}79^+$ vessels, respectively.

Integrin α4β7•IgG heterodimeric chimera *in situ* binding assay

An integrin α4β7•IgG heterodimeric chimera was obtained from the culture medium of human embryonic kidney (HEK) 293T cells transiently cotransfected with pcDNA3.1/Hygro-α4•IgG-FLAG and pcDNA3.1/Hygro-β7•IgG-HA at a 1:1 ratio. Culture media was concentrated ~10-fold using Centriprep YM30 (Millipore, Billerica, MA), as described previously.[32] After blocking with Dulbecco's modified Eagle's medium (DMEM) supplemented with 10% fetal bovine serum (FBS) (HyClone, South Logan, UT) for 20 min, tissues sections were incubated for 30 min with the integrin α4β7•IgG heterodimeric chimera in the same media supplemented with 20 mM HEPES (pH 7.0) and 1 mM $MnCl_2$. After washing with DMEM, tissues were incubated with anti-FLAG monoclonal antibody M2 (Sigma-Aldrich) diluted 1:100 for 30 min followed by a 30-min incubation with Alexa Fluor 488-labeled goat anti-mouse IgG (Invitrogen, Carlsbad, CA). Tissues were mounted with Vectashield mounting medium (Vector Laboratories, Burlingame, CA) and observed under an AX-80 fluorescence microscope (Olympus). Negative control experiments were done using DMEM supplemented with 5 mM EDTA throughout the procedure to chelate divalent cations.

Statistical analysis

Differences among groups were statistically analyzed by the Kruskal-Wallis test with Dunn's post-test using GraphPad Prism 6 software (GraphPad Software, San Diego, CA). *P* values less than 0.05 were considered significant.

RESULTS

Nodular gastritis and atrophic gastritis tissues exhibit a comparable number of lymphoid follicles

To conduct quantitative analysis to evaluate whether nodular gastritis is characterized by lymphoid follicle hyperplasia, we first determined the number of lymphoid follicles in nodular gastritis and atrophic gastritis . In control normal gastric mucosa, only minimal lymphocyte infiltrate was observed in the lamina propria, and formation of lymphoid follicles was scarcely detected (Fig. 4A). However, in both nodular (Fig. 4B) and atrophic (Fig. 4C) gastritis, we frequently observed formation of lymphoid follicles. As shown in Fig. 5A, the number of lymphoid follicles in both nodular and atrophic gastritis was significantly greater than that seen in normal gastric mucosa in all five biopsy sites; however, this number did not differ significantly between the two types of gastritis.

Lymphoid follicles in nodular gastritis are larger than those in atrophic gastritis

Next, we determined the size of lymphoid follicles in nodular and atrophic gastritis and found that follicles formed in nodular gastritis were larger than those seen in atrophic gastritis (see Fig. 4B, C). Analysis of a total of 195 cases, including normal gastric mucosa, showed that

lymphoid follicle diameter in nodular gastritis was significantly greater than that seen in atrophic gastritis, with particularly high statistical significance ($p < 0.001$) at biopsy sites A1, A2, IA, and B1 (Fig. 5B). Follicle diameter in atrophic gastritis was comparable to that seen in normal gastric mucosa, except at biopsy site IA, where inflammation is generally more prominent than it is in other biopsy sites.[33] We then compared occupancy, defined as the ratio of follicle diameter to mucosal thickness (see Fig. 3, left panel), between nodular and atrophic gastritis. As shown in Fig. 6A, except for biopsy site B2, the follicle occupancy ratio in nodular gastritis was never less than 0.64 and was greater than that in atrophic gastritis (which did not exceed 0.51) with high statistical significance ($p < 0.001$). These findings indicate that appearance of enlarged hyperplastic lymphoid follicles is a histological characteristic of nodular gastritis.

Lymphoid follicles are located more superficially in nodular compared to atrophic gastritis

We then compared the location of lymphoid follicles between nodular and atrophic gastritis. As indicated schematically in Fig. 3 (right panel), the smaller the A/B ratio, the more superficially located is a lymphoid follicle. Lymphoid follicles in nodular gastritis were

located more superficially than those observed in atrophic gastritis except at biopsy site B2 (Fig. 6B), suggesting that superficial position of lymphoid follicles is an additional indicator of nodular gastritis.

MAdCAM-1$^+$ HEV-like vessels are induced in both nodular and atrophic gastritis

We next focused on HEV-like vessels observed in nodular and atrophic gastritis. In both cases, a portion of CD34$^+$ vessels were morphologically similar to HEVs in secondary lymphoid organs (Fig. 7, top rows), and these HEV-like vessels were also positive for MAdCAM-1. Such MAdCAM-1$^+$ HEV-like vessels were scarcely detected in normal gastric mucosa (Fig. 7, middle rows). MAdCAM-1$^+$ HEV-like vessels may function in recruitment of memory lymphocytes, because they were bound by an integrin $\alpha4\beta7$•IgG heterodimeric chimera in a divalent cation-dependent fashion (Fig. 8). Interestingly, as shown in Fig. 9A, while the percentage of MAdCAM-1$^+$ HEV-like vessels in both nodular and atrophic gastritis exceeded that seen in normal gastric mucosa with high statistical significance ($p < 0.001$), the percentage did not differ significantly between the two gastritis conditions except at biopsy site IA, where, as noted, inflammation is generally more prominent than it is at other biopsy sites.[33] This finding suggests that MAdCAM-1 is

induced on venular endothelial cells in the gastric lamina propria regardless of the type of chronic gastritis, and thus this protein may not directly contribute to the unique pathogenesis of nodular gastritis.

MECA-79$^+$ HEV-like vessels are preferentially induced in areas of nodular gastritis

As was the case with MAdCAM-1$^+$ HEV-like vessels, a portion of CD34$^+$ vessels was positive for MECA-79 in both types of gastritis, while MECA-79$^+$ HEV-like vessels were hardly detected in normal gastric mucosa (Fig. 7, bottom rows). Interestingly, unlike MAdCAM-1$^+$ HEV-like vessels, the percentage of MECA-79$^+$ HEV-like vessels in nodular gastritis was greater than that seen in both normal gastric mucosa and atrophic gastritis with high statistical significance ($p < 0.001$) at biopsy sites A1, A2 and IA (Fig. 9B), which precisely match the appearance of gooseflesh seen in endoscopic observation of nodular gastritis.

DISCUSSION

In the present study, we demonstrate that superficially-located, enlarged hyperplastic lymphoid follicles histologically characterize nodular gastritis, and that these follicles correspond to nodular and/or granular lesions resembling gooseflesh, which are observed endoscopically. It is accepted that the characteristic histological finding of nodular gastritis is hyperplasia of lymphoid follicles;[2,3,8] however, quantitative analysis of nodular gastritis focusing on lymphoid follicles has not been reported. To the best of our knowledge, this is the first such analysis employing a substantial number of nodular gastritis samples.

Here we show that the percentage of MAdCAM-1^+ HEV-like vessels in both nodular and atrophic gastritis was significantly greater than that seen in normal gastric mucosa, while this percentage did not differ significantly between the two types of gastritis, suggesting that MAdCAM-1 protein does not preferentially contribute to the pathogenesis of nodular gastritis. This finding is inconsistent with a report by Ohara *et al*. who demonstrated that the percentage of MAdCAM-1^+ vessels in nodular gastritis was significantly greater than that seen in *H. pylori*-positive controls.[4] This lack of agreement could be due to the fact that the *H. pylori*-positive controls used in that study may have had only a mild chronic inflammation or to differences in sample size.

We also found that the percentage of MECA-79$^+$ HEV-like vessels in nodular gastritis was greater than that in atrophic gastritis with high statistical significance at the biopsy sites A1, A2 and IA, where endoscopic gooseflesh appearance is evident. This finding agrees with previous reports demonstrating that samples obtained from the gastric corpus show far less inflammation and fewer lymphoid follicles compared to antral biopsies.[11,34]

We also demonstrated that MAdCAM-1 proteins expressed on HEV-like vessels are functional, since an integrin α4β7•IgG heterodimeric chimera bound to these vessels in a divalent cation-dependent manner. We also performed L-selectin•IgM chimera *in situ* binding assay but did not detect signals in the samples tested (data not shown). In our previous study of chronic *H. pylori* gastritis, only a fraction of HEV-like vessels were bound by the L-selectin•IgM chimera.[20] These results suggest that interaction between L-selectin and 6-sulfo sLeX contributes in only a limited manner to lymphocyte recruitment in gastric MALT, and that the interaction of integrin α4β7 in its low-affinity state with MAdCAM-1 is important primarily for the "rolling" step of lymphocyte recruitment.

Kamada *et al*. have reported a possible association between nodular gastritis and diffuse-type gastric carcinoma, including signet-ring cell carcinoma.[6] Indeed, among 99

nodular gastritis cases examined here, one patient also had signet-ring cell carcinoma. It is now evident that development of diffuse-type carcinoma is closely related to *H. pylori* infection;[35,36] however, earlier it was thought that this carcinoma had little relation to *H. pylori* infection because atrophic changes seen in these patients were not severe in the area adjacent to the tumor.[37,38] Since atrophic changes are usually inconspicuous in nodular gastritis, we speculate that diffuse-type gastric carcinoma may develop during progression from nodular to atrophic gastritis.[37,38] Further studies are required to clarify nodular gastritis-associated pathogenesis of diffuse-type gastric carcinoma.

Acknowledgements: We thank Dr. Jun Nakayama for encouragement, Ms. Yoshiko Sato for technical assistance, and Dr. Elise Lamar for critical reading of the manuscript.

Conflicts of interest and sources of funding: This work was supported in part by a Grant-in-Aid for Scientific Research 24590410 from the Japan Society for the Promotion of Science (to MK). The authors state that there are no conflicts of interests to disclose.

References

1. Kamada T, Hata J, Tanaka A, Kusunoki H, Miyamoto M, Inoue K, Sadahira Y, Haruma K. Nodular gastritis and gastric cancer. *Dig Endosc* 2006; 18: 79-83.

2. De Giacomo C, Flocca R, Villani L, Licardi G, Diegoli N, Danadini A, Maggiore G. *Helicobacter pylori* infection and chronic gastritis: clinical, serological, and histologic correlations in children treated with amoxicillin and colloidal bismuth subcitrate. *J Pediatr Gastroenterol Nutr* 1990; 11: 310-6.

3. Miyamoto M, Haruma K, Yoshihara M, Hiyama T, Sumioka M, Nishisaka T, Tanaka S, Chayama K. Nodular gastritis in adults is caused by *Helicobacter pylori* infection. *Dig Dis Sci* 2003; 48: 968-75.

4. Ohara H, Isomoto H, Wen CY, Ejima C, Murata M, Miyazaki M, Takeshima F, Mizuta Y, Murata I, Koji T, Nagura H, Kohno S. Expression of mucosal addressin cell adhesion molecule 1 on vascular endothelium of gastric mucosa in patients with nodular gastritis. *World J Gastroenterol* 2003; 9: 2701-5.

5. Kitamura S, Yasuda M, Muguruma N, Okamoto K, Takeuchi H, Bando Y, Miyamoto H, Okahisa T, Yano M, Torisu R, Takayama T. Prevalence and characteristics of nodular gastritis in Japanese elderly. *J Gastroenterol Hepatol* 2013; 28: 1154-60.

6. Kamada T, Tanaka A, Yamanaka Y, Manabe N, Kusunori H, Miyamoto M, Tanaka S, Hata J, Chayama K, Haruma K. Nodular gastritis with *Helicobacter pylori* infection is strongly associated with diffuse-type gastric cancer in young patients. *Dig Endosc* 2007; 19: 180-4.

7. Li C, Kim S, Lai JF, Hyung WJ, Choi WH, Choi SH, Noh SH. Advanced gastric carcinoma with signet ring cell histology. *Oncology* 2007; 72: 64-8.

8. Eastham EJ, Elliott TS, Berkeley D, Jones DM. *Campylobacter pylori* infection in children. *J Infect* 1988; 16: 77-9.

9. Shiotani A, Kamada T, Kumamoto M, Nakae Y, Nakamura Y, Kakudo K, Haruma K. Nodular gastritis in Japanese young adults: endoscopic and histological observations. *J Gastroenterol* 2007; 42: 610-5.

10. Owen DA. Normal histology of the stomach. *Am J Surg Pathol* 1986; 10: 48-61.

11. Genta RM, Hamner HW, Graham DY. Gastric lymphoid follicles in *Helicobacter pylori* infection: frequency, distribution, and response to triple therapy. *Hum Pathol* 1993; 24: 577-83.

12. Drayton DL, Liao S, Mounzer RH, Ruddle NH. Lymphoid organ development: from ontogeny to neogenesis. *Nat Immunol* 2006; 7: 344-53.

13. Butcher EC, Picker LJ. Lymphocyte homing and homeostasis. *Science* 1996; 272: 60-6.

14. Girard JP, Moussion C, Förster R. HEVs, lymphatics and homeostatic immune cell trafficking in lymph nodes. *Nat Rev Immunol* 2012; 12: 762-73.

15. Aloisi F, Pujol-Borrell R. Lymphoid neonegesis in chronic inflammatory diseases. *Nat Rev Immunol* 2006; 6: 205-17.

16. Michie SA, Streeter PR, Bolt PA, Butcher EC, Picker LJ. The human peripheral lymph node vascular addressin. An inducible endothelial antigen involved in lymphocyte homing. *Am J Pathol* 1993; 143: 1688-98.

17. Berlin C, Berg EL, Briskin MJ, Andrew DP, Kilshaw PJ, Holzmann B, Weissman IL, Hamann A, Butcher EC. α4β7 integrin mediates lymphocyte binding to the mucosal vascular addressin MAdCAM-1. *Cell* 1993; 74: 185-95.

18. Kobayashi M, Hoshino H, Suzawa K, Sakai Y, Nakayama J, Fukuda M. Two distinct lymphocyte homing systems involved in the pathogenesis of chronic inflammatory gastrointestinal diseases. *Semin Immunopathol* 2012; 34: 401-13.

19. Streeter PR, Rouse BT, Butcher EC. Immunohistologic and functional characterization of a vascular addressin involved in lymphocyte homing into peripheral lymph nodes. *J Cell Biol* 1988; 107: 1853-62.

20. Kobayashi M, Mitoma J, Nakamura N, Katsuyama T, Nakayama J, Fukuda M. Induction of peripheral lymph node addressin in human gastric mucosa infected by *Helicobacter pylori*. *Proc Natl Acad Sci U S A* 2004; 101: 17807-12.

21. Suzawa K, Kobayashi M, Sakai Y, Hoshino H, Watanabe M, Harada O, Ohtani H, Fukuda M, Nakayama J. Preferential induction of peripheral lymph node addressin on high endothelial venules in the active phase of ulcerative colitis. *Am J Gastroenterol* 2007; 102: 1499-509.

22. Kobayashi M, Hoshino H, Masumoto J, Fukushima M, Suzawa K, Kageyama S, Suzuki M, Ohtani H, Fukuda M, Nakayama J. GlcNAc6ST-1-mediated decoration of MAdCAM-1 protein with L-selectin ligand carbohydrates directs disease activity of ulcerative colitis. *Inflamm Bowel Dis* 2009; 15: 697-706.

23. Maruyama M, Kobayashi M, Sakai Y, Hiraoka N, Ohya A, Kageyama S, Tanaka E, Nakayama J, Morohoshi T. Periductal induction of high endothelial venule-like vessels in type 1 autoimmune pancreatitis. *Pancreas* 2013; 42: 53-9.

24. Yeh JC, Hiraoka N, Petryniak B, Nakayama J, Ellies LG, Rabuka D, Hindsgaul O, Marth JD, Lowe JB, Fukuda M. Novel sulfated lymphocyte homing receptors and their control by a core 1 extension β1,3-*N*-acetylglucosaminyltransferase. *Cell* 2001; 105: 957-69.

25. Uchimura K, Rosen SD. Sulfated L-selectin ligands as a therapeutic target in chronic inflammation. *Trends Immunol* 2006; 27: 559-65.

26. Briskin M, Winsor-Hines D, Shyjan A, Cochran N, Bloom S, Wilson J, McEvoy LM, Butcher EC, Kassam N, Mackay CR, Newman W, Ringler DJ. Human mucosal addressin cell adhesion molecule-1 is preferentially expressed in intestinal tract and associated lymphoid tissue. *Am J Pathol* 1997; 151: 97-110.

27. Berg EL, McEvoy LM, Berlin C, Bargatze RF, Butcher EC. L-selectin-mediated lymphocyte rolling on MAdCAM-1. *Nature* 1993; 366: 695-8.

28. Bargatze RF, Jutila MA, Butcher EC. Distinct roles of L-selectin and integrins α4β7 and LFA-1 in lymphocyte homing to Peyer's patch-HEV in situ: the multistep model confirmed and refined. *Immunity* 1995; 3: 99-108.

29. Dixon MF, Genta RM, Yardley JH, Correa P. Classification and grading of gastritis. The updated Sydney system. *Am J Surg Pathol* 1996; 20: 1161-81.

30. Sado Y, Inoue S, Tomono Y, Omori H. Lymphocytes from enlarged iliac lymph nodes as fusion partners for the production of monoclonal antibodies after a single tail base immunization attempt. *Acta Histochem Cytochem* 2006; 39: 89-94.

31. Kobayashi M, Nakayama J. Immunohistochemical analysis of carbohydrate antigens in

chronic inflammatory gastrointestinal diseases. *Methods Enzymol* 2010; 479: 271-89.

32. Hoshino H, Kobayashi M, Mitoma J, Sato Y, Fukuda M, Nakayama J. An integrin α4β7•IgG heterodimeric chimera binds to MAdCAM-1 on high endothelial venules in gut-associated lymphoid tissue. *J Histochem Cytochem* 2011; 59: 572-83.
33. Van Zanten SJ, Dixon MF, Lee A. The gastric transitional zones: neglected links between gastroduodenal pathology and *Helicobacter* ecology. *Gastroenterology* 1999; 116: 1217-29.
34. Sbeih F, Abdullah A, Sullivan S, Merenkov Z. Antral nodularity, gastric lymphoid hyperplasia, and *Helicobacter pylori* in adults. *J Clin Gastroenterol* 1996; 22: 227-30.
35. Kikuchi S, Wada O, Nakajima T, Nishi T, Kobayashi O, Konishi T, Inaba Y. Serum anti-*Helicobacter pylori* antibody and gastric carcinoma among young adults. *Cancer* 1995; 75: 2789-93.
36. Kokkola A, Valle J, Haapiainen R, Sipponen P, Kivilaakso E, Puolakkainen P. *Helicobacter pylori* infection in young patients with gastric carcinoma. *Scand J Gastroenterol* 1996; 31: 643-7.
37. Sipponen P, Kosunen TU, Valle J, Riihelä M, Seppälä K. *Helicobacter pylori* infection and chronic gastritis in gastric cancer. *J Clin Pathol* 1992; 45: 319-23.

38. Uemura N, Okamoto S, Yamamoto S, Matsumura N, Yamaguchi S, Yamakido M, Taniyama K, Sasaki N, Schlemper RJ. *Helicobacter pylori* infection and the development of gastric cancer. *N Engl J Med* 2001; 345: 784-9.

Figure legends

Fig. 1 Representative endoscopic appearance of nodular gastritis (A, B) and atrophic gastritis (C). (A) Multiple small nodular or granular lesions resembling gooseflesh are observed in the gastric antrum. (B) The gooseflesh appearance is highlighted after spraying tissue with a solution containing indigo carmine stain. (C) Gastric rugae are flattened and submucosal vascular patterns are visible in the distended stomach.

Fig. 2 Specificity of human MAdCAM-1 monoclonal antibody (clone #15-8G-61) as assessed by immunohistochemistry (A), flow cytometry (B) and Western blot analysis (C). (A) HEVs in human mesenteric lymph nodes were specifically decorated by #15-8G-61. Bar, 100 μm. (B) #15-8G-61 specifically recognizes CHO cells stably expressing human MAdCAM-1 (CHO/MAdCAM-1) (gray histogram). White dotted histogram represents background staining to parental CHO cells. (C) Western blot analysis demonstrates a single band at ~82 kDa, corresponding to a glycosylated species of human MAdCAM-1.

Fig. 3 Schematic representation showing how occupancy (left panel) and location (right panel) of lymphoid follicles were assessed. (Left panel) Occupancy is reported as the A/B

ratio, where A is follicle diameter perpendicular to muscularis mucosae and B is mucosal thickness (distance between the apical surface of foveolar epithelium to the upper face of muscularis mucosae). (Right panel) Location is quantified by the ratio A/B, where A is the distance between the apical surface of foveolar epithelium and the center of lymphoid follicle, and B is mucosal thickness. In terms of location, the smaller the A/B value, the more superficially a lymphoid follicle is located. FE, foveolar epithelium; LF, lymphoid follicle; MM, muscularis mucosae.

Fig. 4 Representative histology of normal gastric mucosa (A), nodular gastritis (B), and atrophic gastritis (C). Lymphoid follicles form in the gastric lamina propria of nodular gastritis and atrophic gastritis. Note that the size of the lymphoid follicle seen in nodular gastritis is greater than that seen in atrophic gastritis. Hematoxylin and eosin (H&E) stain. Bar, 200 μm.

Fig. 5 Comparison of the number (A) and diameter (B) of lymphoid follicles among samples of nodular gastritis, atrophic gastritis, and normal gastric mucosa. Five biopsy sites are indicated as A1, A2, IA, B1 and B2, respectively, based on the updated Sydney system.

Data are expressed as mean ± SEM. *, $p < 0.05$; ***, $p < 0.001$; NS, not significant.

Fig. 6 Comparison of occupancy (A) and location (B) of lymphoid follicles in nodular gastritis and atrophic gastritis. Five biopsy sites are indicated as A1, A2, IA, B1 and B2, respectively, based on the updated Sydney system. Data are expressed as mean ± SEM. **, $p < 0.01$; ***, $p < 0.001$; NS, not significant.

Fig. 7 HEV-like vessels observed in nodular gastritis and atrophic gastritis. HEV-like vessels were immunostained for CD34, MAdCAM-1 or MECA-79. Normal gastric mucosa lacks HEV-like vessels. Bar, 100 μm.

Fig. 8 Integrin α4β7•IgG heterodimeric chimera *in situ* binding assay. Frozen stomach tissues with nodular gastritis were probed with an integrin α4β7•IgG heterodimeric chimera in the absence (left panel) or presence (right panel) of 5 mM EDTA to chelate divalent cations. Green fluorescence signals represent integrin α4β7•IgG heterodimeric chimera binding. Bar, 50 μm.

Fig. 9 Comparison of the percentage of MAdCAM-1^+ (A) and MECA-79^+ (B) HEV-like vessels among samples of nodular gastritis, atrophic gastritis, and normal gastric mucosa. Five biopsy sites are indicated as A1, A2, IA, B1 and B2, respectively, based on the updated Sydney system. Data are expressed as mean ± SEM. **, $p < 0.01$; ***, $p < 0.001$; NS, not significant.

Table 1 Clinical characteristics of patients

	Nodular gastritis (*n* = 99)	Atrophic gastritis (*n* = 65)	Normal (*n* = 31)
Sex (*n*, %)			
Male	39 (39.3)	24 (36.9)	9 (29.0)
Female	60 (60.6)	41 (63.1)	22 (71.0)
Age (years)			
Mean ± SD	28.9 ± 16.9	51.8 ± 16.3	42.5 ± 21.4
Range	4 - 79	16 - 82	11 - 79
H. pylori infection (*n*, %)	99 (100)	65 (100)	0 (0)

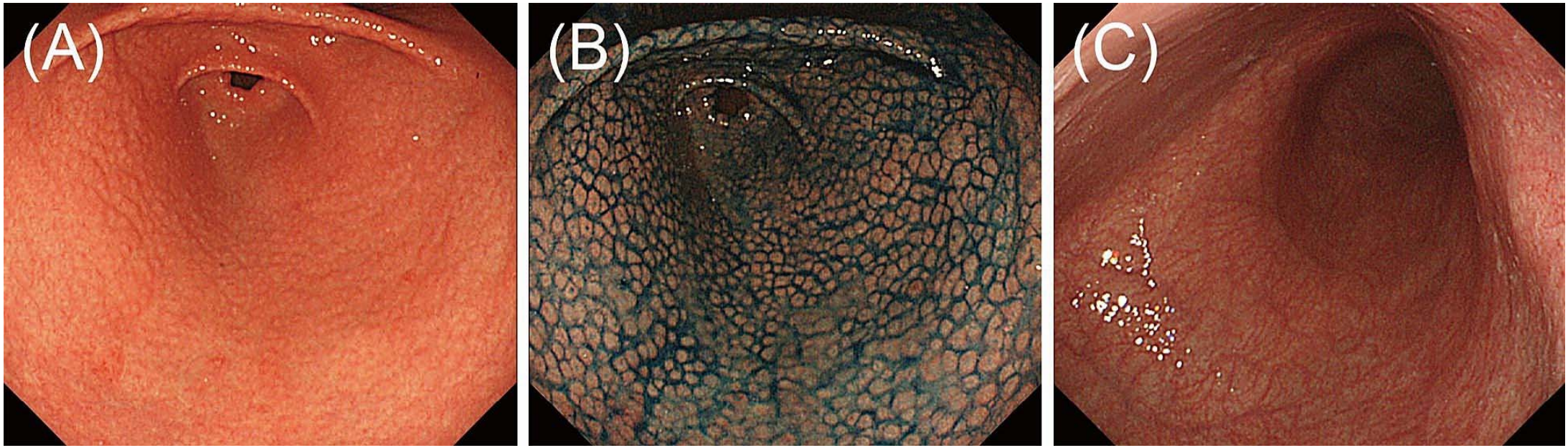
(A)
(B)
(C)

(A)

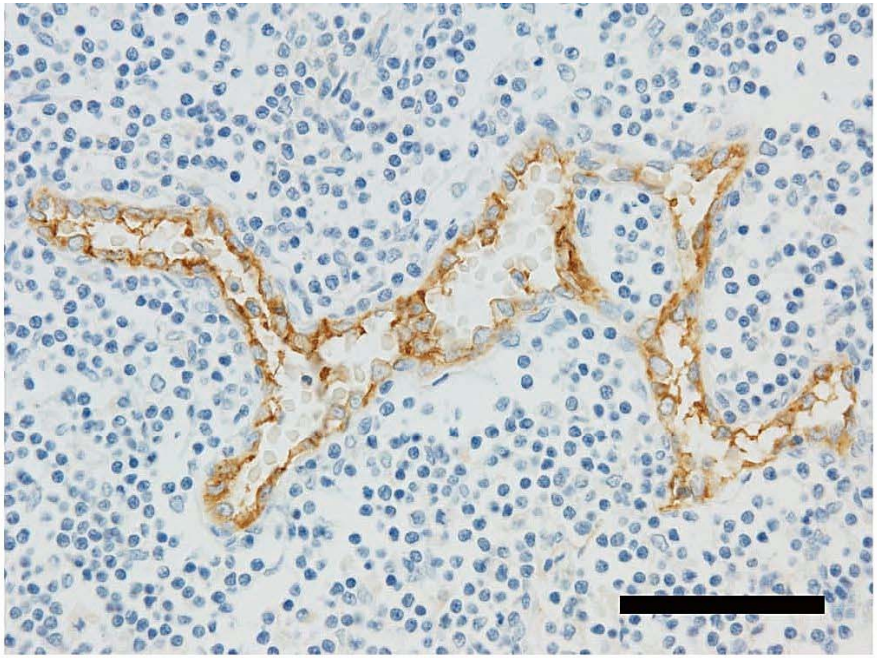

(B)

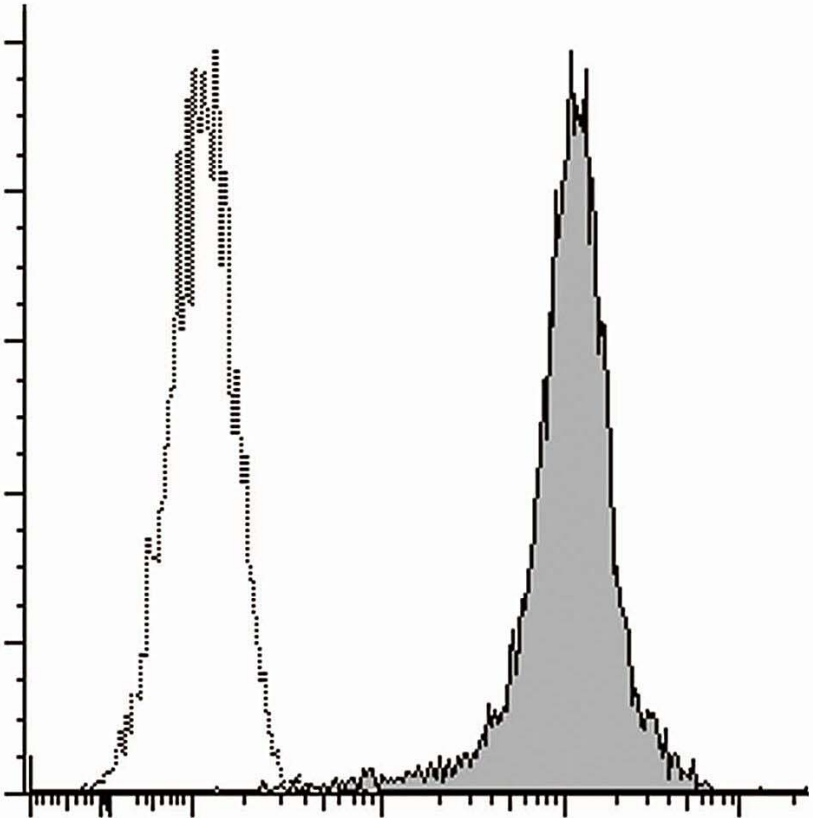

(C)

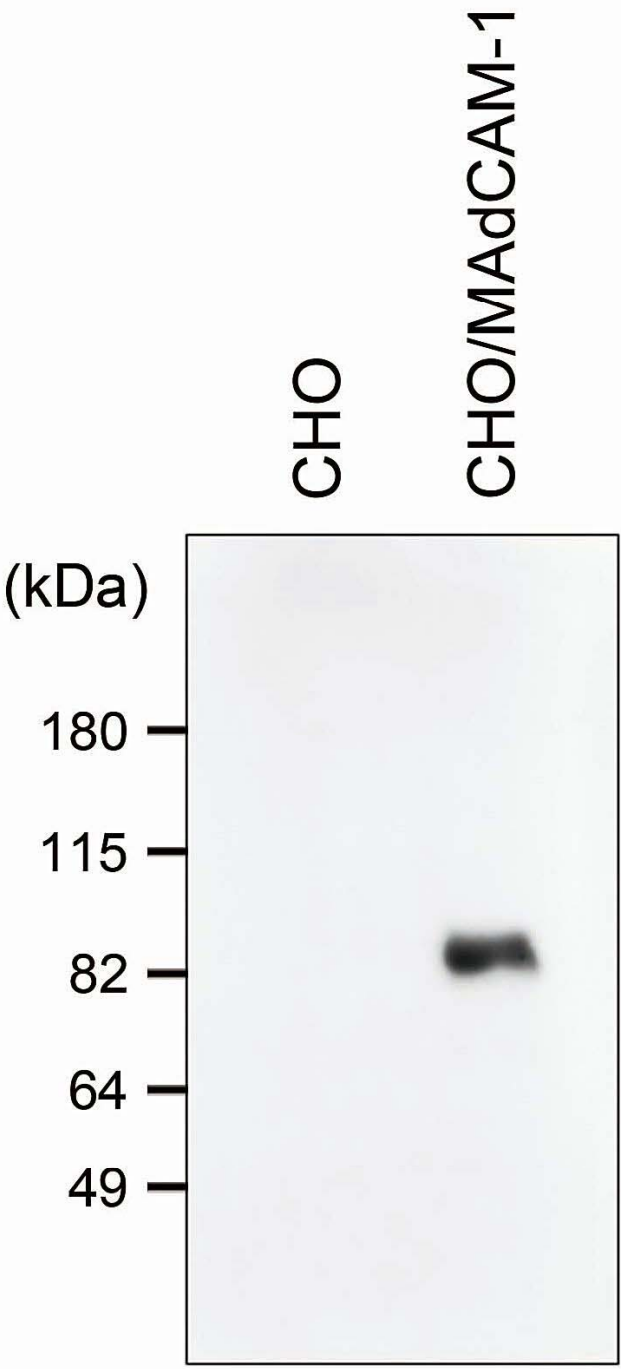

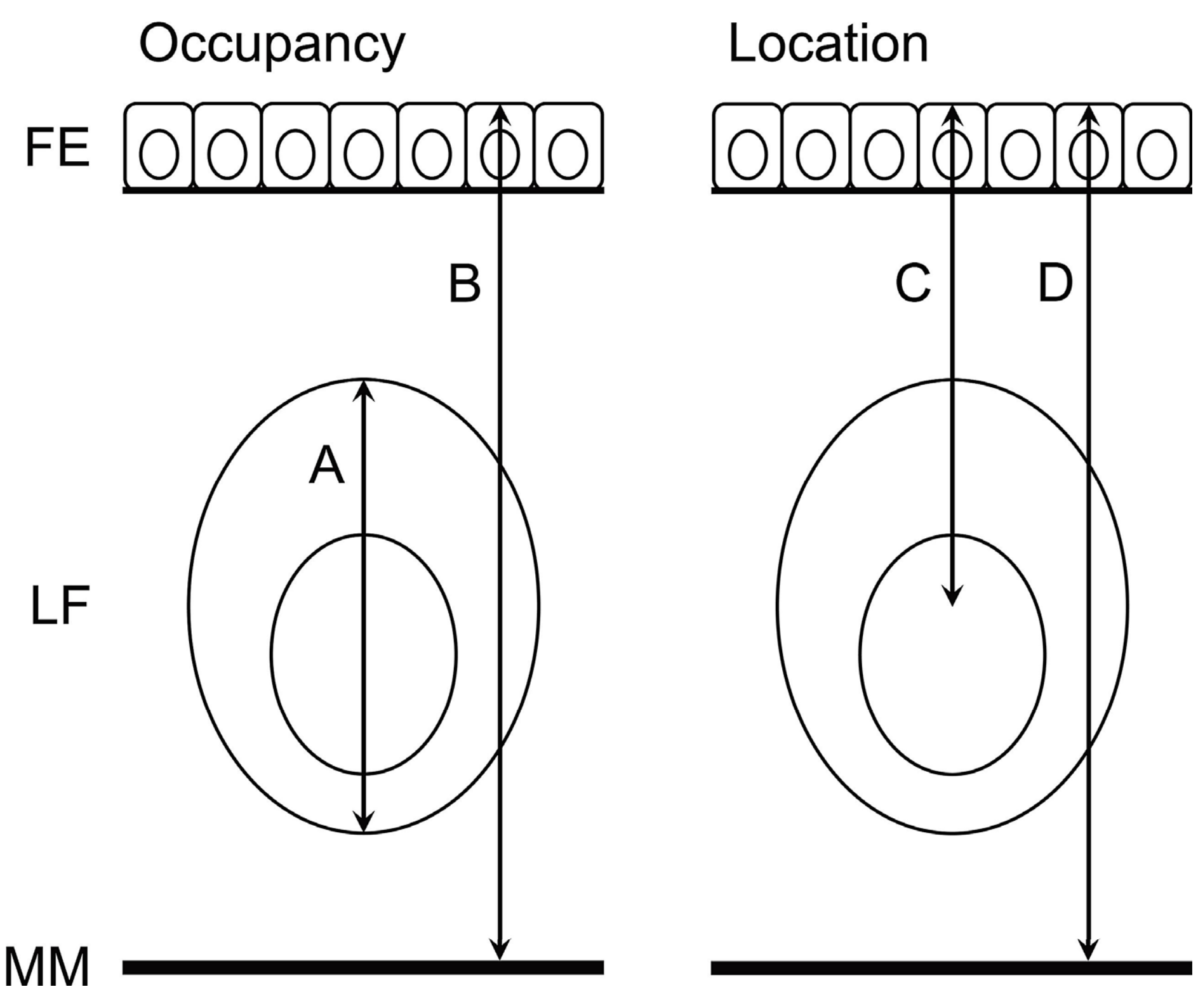
Occupancy
Location
FE
B
C
D
A
LF
MM

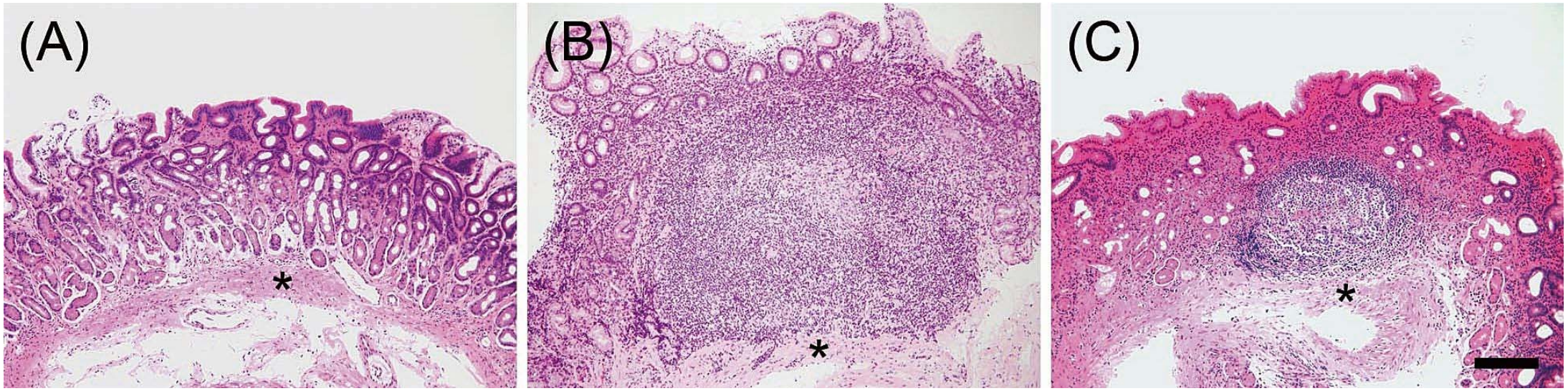
(A)
*
(B)
*
(C)
*

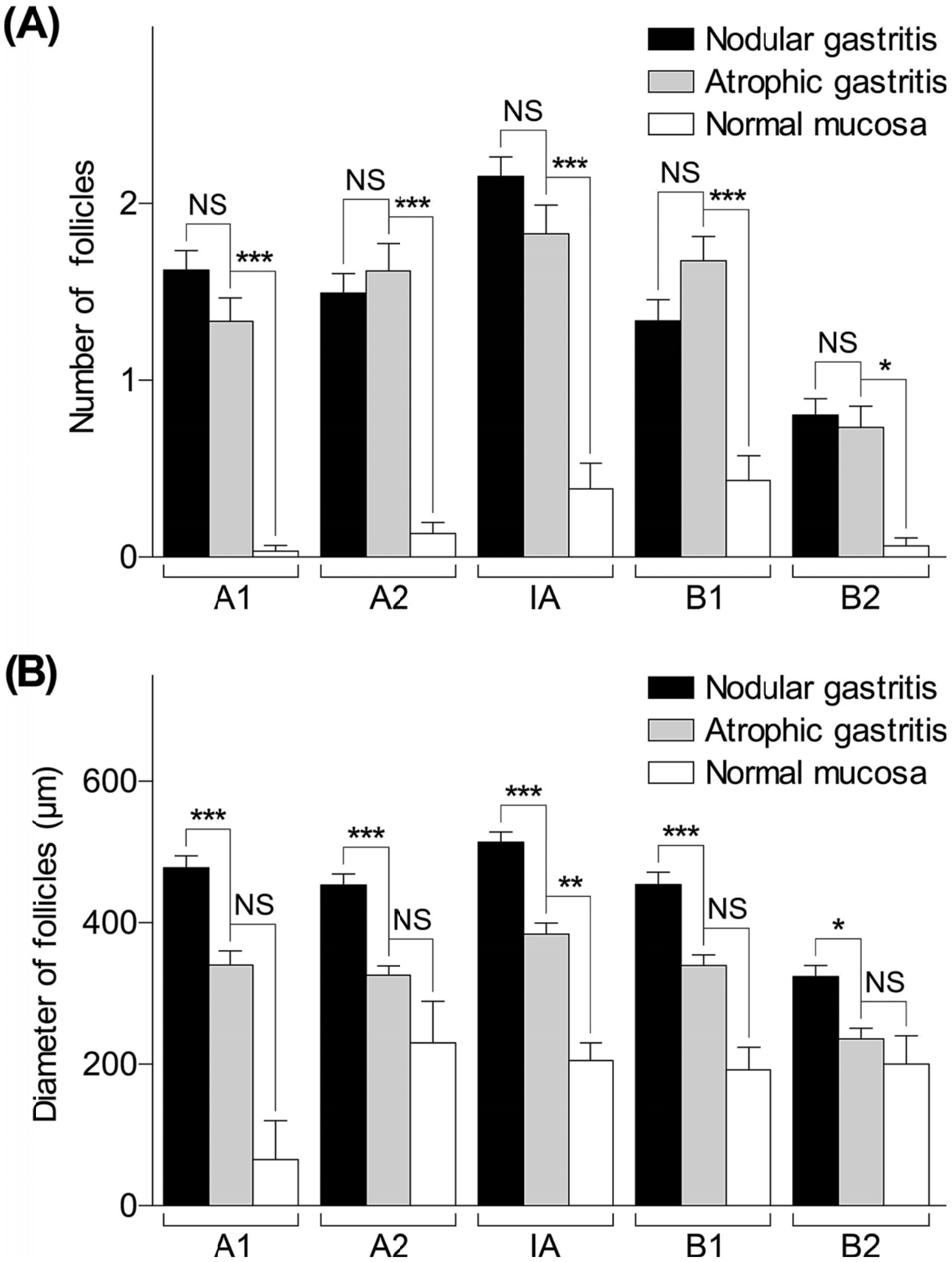
(A)
Nodular gastritis
Atrophic gastritis
Normal mucosa
Number of follicles
0
1
2
NS
***
NS
***
NS
***
NS
***
NS
*
A1
A2
IA
B1
B2
(B)
Nodular gastritis
Atrophic gastritis
Normal mucosa
Diameter of follicles (μm)
0
200
400
600
***
NS
***
NS
***
**
***
NS
*
NS
A1
A2
IA
B1
B2

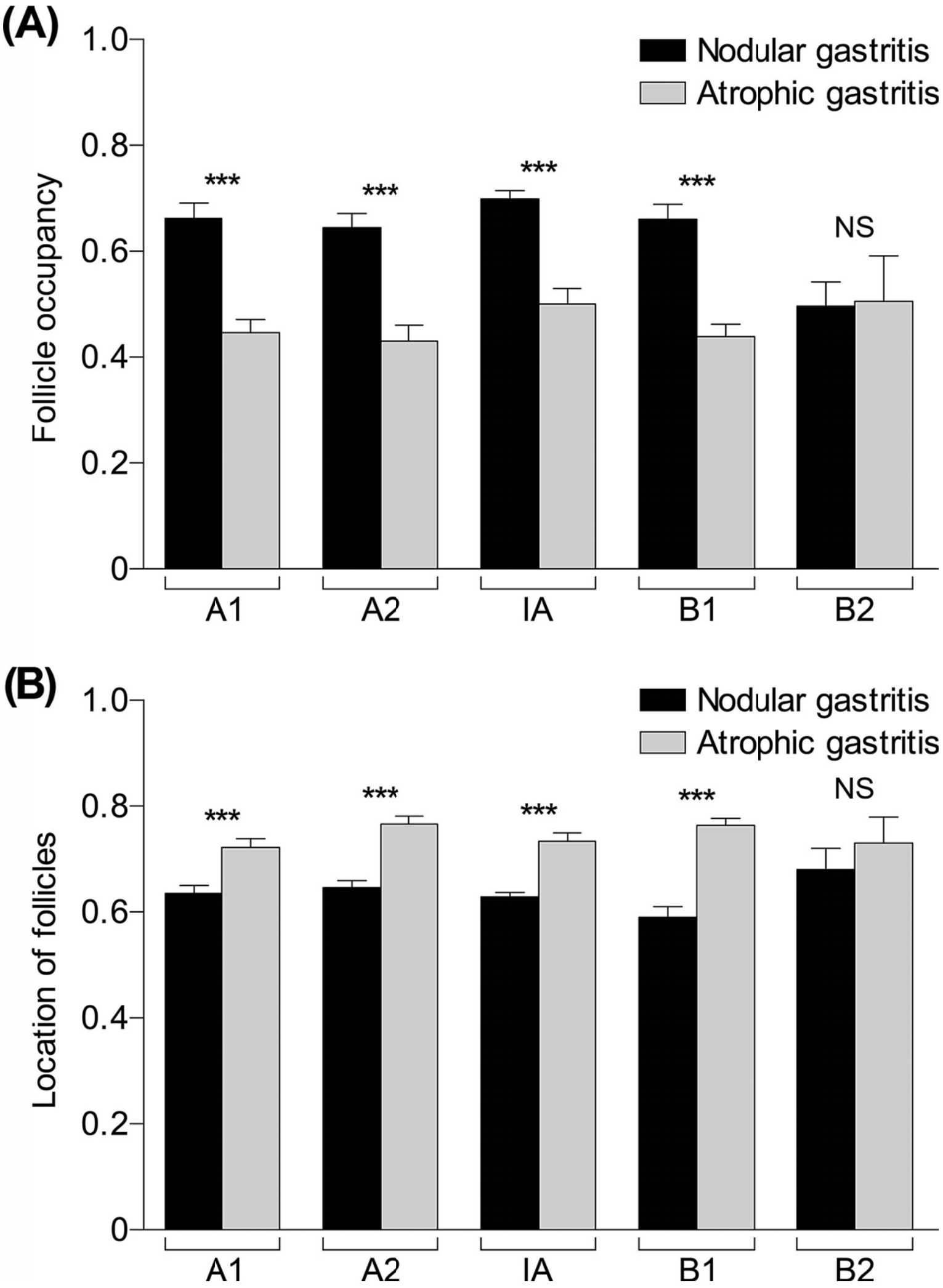
(A)
Nodular gastritis
Atrophic gastritis
Follicle occupancy
1.0
0.8
0.6
0.4
0.2
0
***
***
***
***
NS
A1
A2
IA
B1
B2
(B)
Nodular gastritis
Atrophic gastritis
Location of follicles
1.0
0.8
0.6
0.4
0.2
0
***
***
***
***
NS
A1
A2
IA
B1
B2

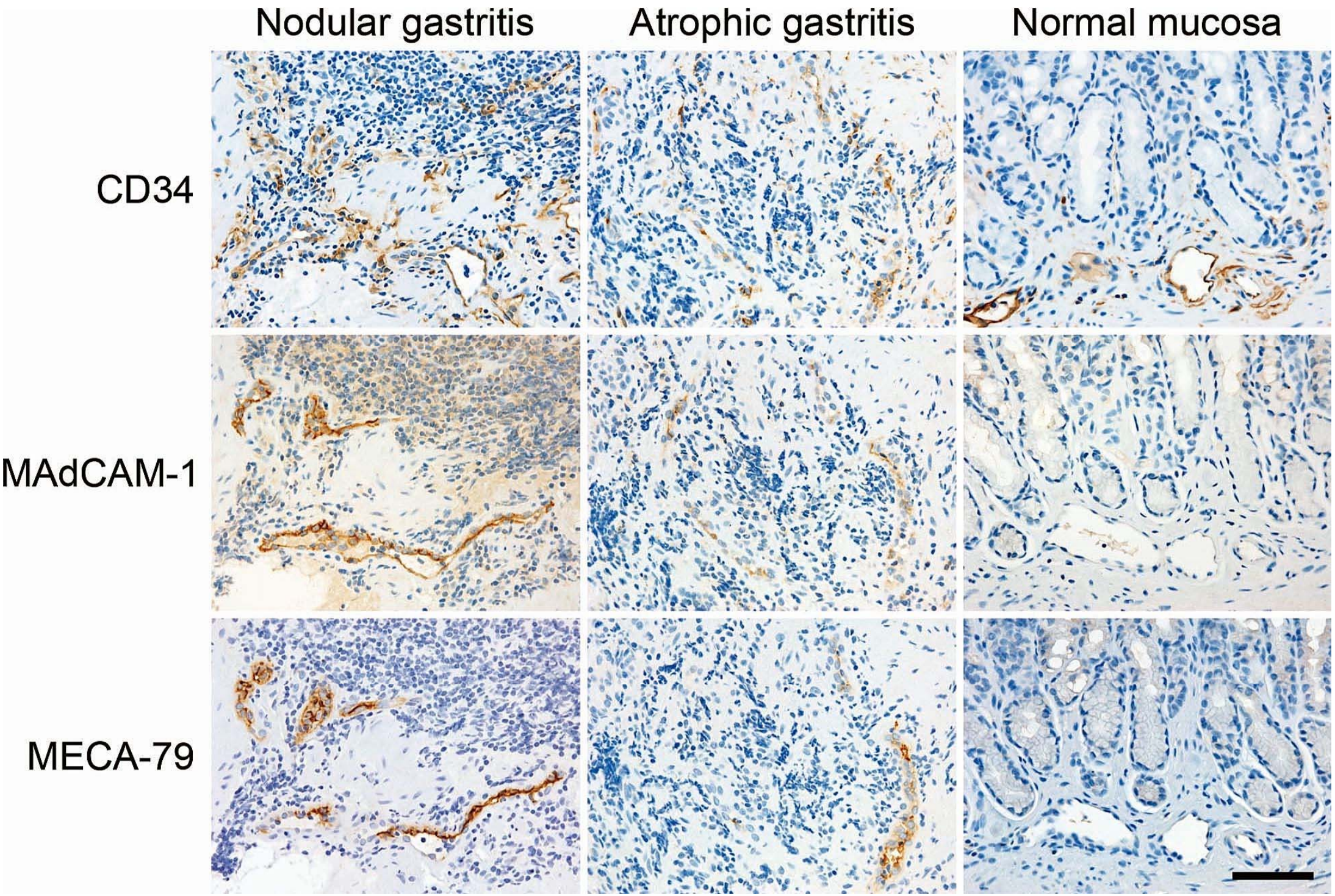
Nodular gastritis
Atrophic gastritis
Normal mucosa
CD34
MAdCAM-1
MECA-79

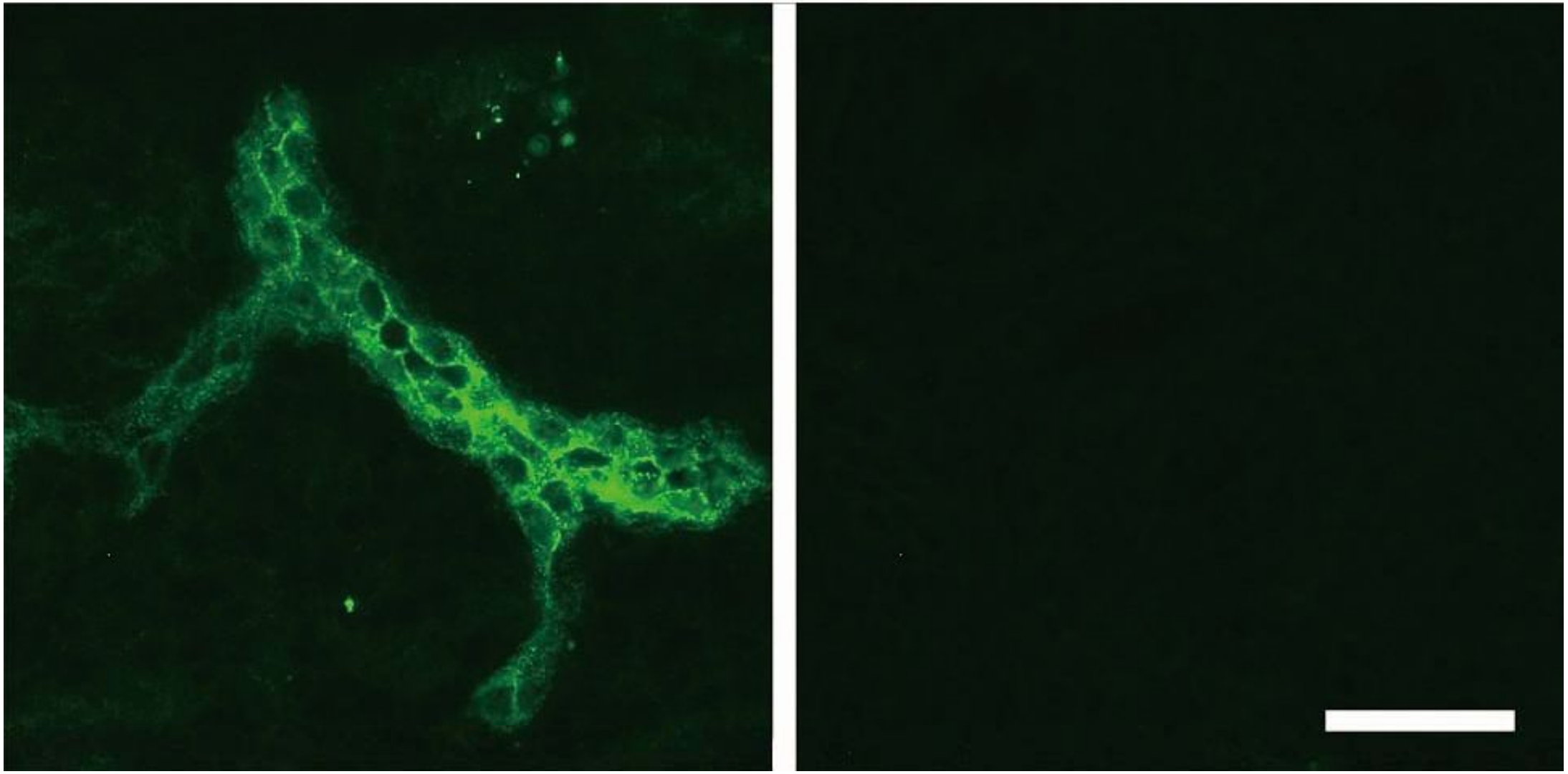
Minus EDTA
Plus EDTA

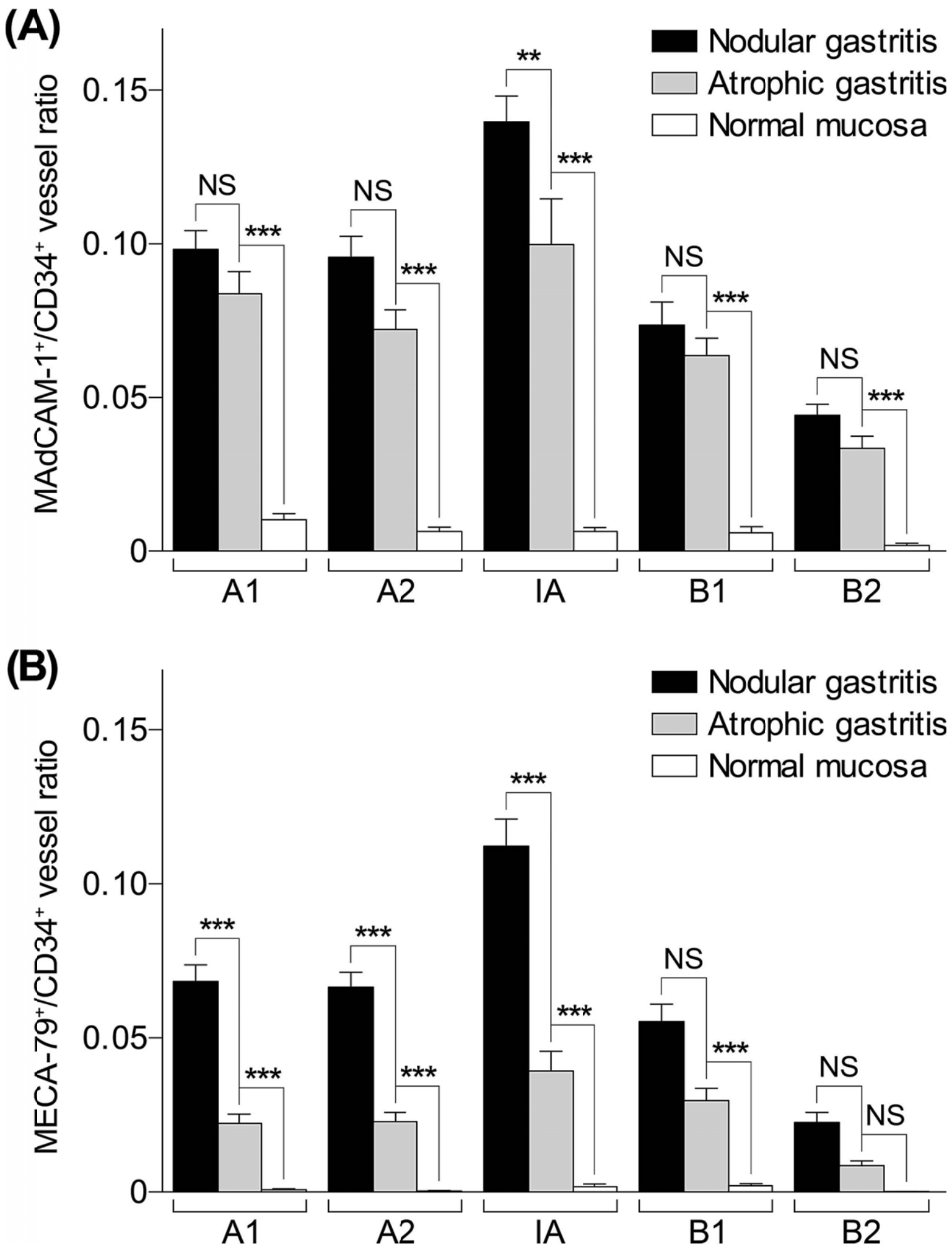
(A)
MAdCAM-1+/CD34+ vessel ratio
0.15
0.10
0.05
0
Nodular gastritis
Atrophic gastritis
Normal mucosa
NS
***
NS
***
**
***
NS
***
NS
***
A1
A2
IA
B1
B2
(B)
MECA-79+/CD34+ vessel ratio
0.15
0.10
0.05
0
Nodular gastritis
Atrophic gastritis
Normal mucosa
***
***
***
***
***
***
NS
***
NS
NS
A1
A2
IA
B1
B2